E 4 Scattering from flowing polymers

P. Lindner

ILL Grenoble

1. Introduction

Application of the neutron scattering technique, in particular at *small angles* (SANS), has considerably advanced the understanding of the structure and dynamics of "soft condensed matter" in the past 20 years. Variable wavelengths and sample-to-detector distances at modern SANS instruments provide a range of momentum transfer which is suitable for studying molecular structures that are between some 1 and 100 nm across. Studies under equilibrium conditions allow one to characterize single molecule parameters and molecular interaction parameters in dilute and concentrated solutions. Other examples are studies of critical phenomena in phase separation, of chain morphology in aggregated systems such as networks and crystalline polymers and characterization of deformation and orientation processes on a molecular level.

The outstanding advantage of this technique is the possibility of isotopic labelling of hydrogen rich compounds, such as synthetic or biological polymers: the difference in neutron scattering lengths of both hydrogen isotopes allows for a "colouring" of molecules by replacement of ^{1}H against ^{2}H. Thus an increased contrast is provided in the neutron scattering experiment but the polymer system remains chemically (almost) unchanged. Furthermore, in a neutron experiment there are fewer restrictions with respect to optical cleanness of the solution (dust problem in light scattering, LS), transparency of container material and absorption (a problem in small angle X-ray scattering, SAXS). However, all three methods (SANS, SAXS, LS) are in principle complementary for structure determination.

This contribution illustrates a quite novel application of the "classical" SANS technique to liquid systems under non-equilibrium conditions (Oberthür, 1983, 1984) which has been developed during the last decade for instance at the Institut Laue-Langevin (ILL) in Grenoble. *Flow fields* in particular are often encountered in process engineering and application of polymeric or colloidal material. There is a fundamental interest in understanding the microscopic structure and dynamics of such "complex fluids" as the macroscopic material properties might change considerably with application of an external perturbation (e.g. non-Newtonian flow behaviour). The technological and practical implications of such studies become immediately evident when we look for instance at injection moulding with polymeric melts, polymer fibre- and foil-extrusion, modern dispersion paints, flocculation, coating techniques or enhanced oil recovery. It is obvious that an "on-line" scattering study with *flowing* systems gives insight into a very realistic state of matter since those processes involve *non-equilibrium* rather than equilibrium states.

The investigation of polymer solutions in laminar shear flow has been chosen here as an example for illustrating the various possibilities which are offered by the SANS technique under non-equilibrium conditions. The concise treatment of scattering theory can be found in standard

references (Guinier & Fournet, 1955; Alexander, 1969; Chen, Chu & Nossal, 1981; Glatter & Kratky, 1982; Lindner & Zemb, 1991; Baruchel et al., 1993; Brumberger, 1995). As far as theoretical concepts and experimental studies of polymer solutions in general are concerned, the reader is referred to standard textbooks (Flory, 1953; Tanford, 1961; Flory, 1969; Yamakawa, 1971, Morawetz, 1975; DeGennes, 1979; Doi & Edwards, 1986; DesCloizeaux & Jannink, 1990, Higgins & Benoît, 1994) and references given therein. A recent ACS symposium series deals with flow induced structure in polymers (Nakatani & Dadmun, 1995)

1.1. NON-EQUILIBRIUM SAMPLE ENVIRONMENT

In what follows we are concerned with small angle neutron scattering (SANS) experiments using "cold" neutrons, whose wavelengths are in the range between 0.45 and 2.0 nm. The high penetrating power of neutrons into matter allows for typical sample thicknesses of the order of 1 to 5 mm, with a typical beam cross section of the order of 0.5 to 1 cm^2. These
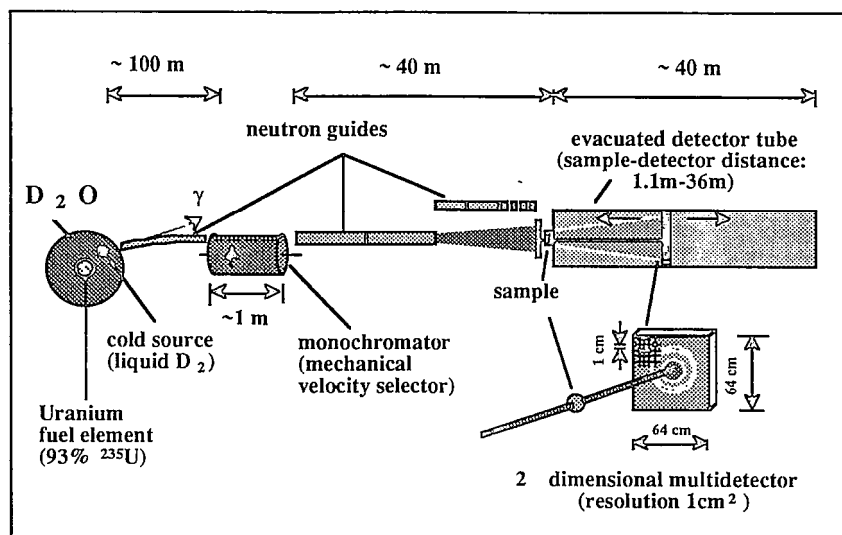

Figure 1. Schematic view of the small-angle neutron scattering instrument D11 at the ILL (Schmatz, Springer, Schelten & Ibel, 1974; Ibel, 1976; Lindner, May & Timmins, 1992).

macroscopic dimensions hence facilitate handling of the sample and its alignment with respect to the beam path. If the sample is a liquid, it will be confined in a quartz cell with defined path length or another material transparent to neutrons (e.g. Vanadium). In a standard SANS experiment the sample will usually be in thermodynamic equilibrium with its environment, at given chemical composition (concentration), pressure and temperature. *Without* external constraints, the scattered intensity (e.g. from a dissolved macromolecule) is a result of the space and time average of all molecular conformations and orientations and an (azimuthally) isotropic scattering pattern is observed on a two dimensional multidetector (cf. Fig. 1).
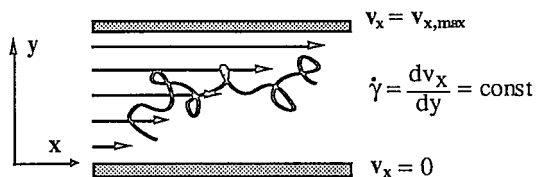
$$v_x = v_{x,max}$$

$$\dot\gamma = \frac{dv_x}{dy} = const$$

$$v_x = 0$$

Figure 2. An example for a hydrodynamic field: a constant, transverse gradient $\dot\gamma$ is acting between two parallel plates (plane Couette flow) on a sheared fluid containing polymer molecules.

Under non-equilibrium conditions in general, an external field is applied to the sample during the scattering experiment. By submitting the sample to external constraints such as *magnetic*, *electric*, or *hydrodynamic fields* (cf. Fig. 2) structural changes can be induced.
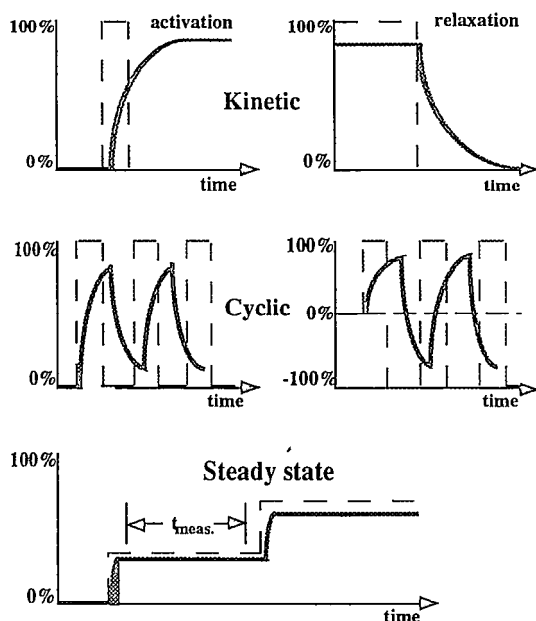

Figure 3.
Some possibilities for kinetic, periodically cyclic and steady state modes of non-equilibrium experiments. The dashed line represents the perturbation of the system by an externally applied field. Note that in a steady state experiment the system is usually exposed to a constant perturbation during the measuring time (e.g. measurement at constant flow velocity in a hydrodynamic field).

Furthermore, various fields can be imposed in different modes of operation as shown schematically in Fig. 3. (i) Thus, in a *kinetic* experiment, an activation process of the sample can be studied after a short perturbation pulse (dashed line), or it is allowed to relax back to equilibrium after an externally imposed perturbation of its equilibrium configuration (relaxation). (ii) In a *cyclic* experiment the sample is periodically distorted around its equilibrium state. (iii) A third type of non-equilibrium experiment is the *steady-state* experiment with keeping the external constraint constant during the measuring time t_{meas}.

Particularly interesting are SANS studies under *steady-state flow*, because of their technological implications. The solute particles of a liquid sample exposed to a hydrodynamic field experience forces due to viscous drag in the streaming fluid which tend to orient, to deform or to order them. The intensity distribution on a two-dimensional multidetector might in this case become anisotropic with respect to the direction of flow. Although complex features, such as viscoelasticity, thixotropy, rheopexy or drag reduction, are well known from (macroscopic) rheological measurements, the underlying (microscopic) mechanisms on the *molecular scale* have

until now not been completely understood and are a matter of intensive research activity both from the experimental and the theoretical point of view (Bird, Armstrong & Hassager, 1977).

1.2. FLOW APPARATUSES FOR SANS

From theoretical aspects as well as for experimental reasons, the linear laminar *Couette flow* is of great importance because of its simplicity. Couette shear flow is given between two parallel plates, one at rest and the other plate moving with constant velocity v_x due to the action of a constant external force. In the case of the *plane* Couette flow the transverse gradient $\dot{\gamma}$ can be written as:

$$\dot{\gamma} = \frac{v_x}{d} = const \tag{1}$$

where d is the distance between the two plates. A practical example is the Couette-type shear apparatus constructed for neutron scattering experiments with liquid systems in a constant shear gradient at the SANS instruments of the Institut Laue-Langevin (cf. Fig. 4; Lindner & Oberthür, 1984).
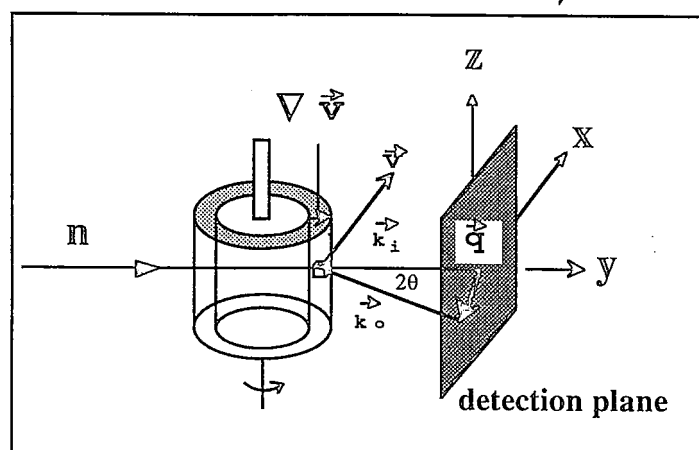

Figure 4. Schematic view of the Couette type shear apparatus used at ILL (Lindner & Oberthür, 1984). The sample is confined in the gap between two concentric quartz cylinders, with the outer one rotating at a constant speed. The inner static cylinder is under temperature control. The incoming primary neutron beam hits the sample normal to the axis of rotation (z-direction) of the outer cylinder and is thus *perpendicular* to the flow v (x-direction) and *parallel* to the shear gradient $\dot{\gamma} = \frac{|v|}{d}$ (y-direction).

The sample container consists of an inner fixed piston and a concentric outer rotating beaker, both made of quartz glass, which is highly transparent for thermal and cold neutrons and shows a very low small angle scattering background. The sample is confined in the annular gap between rotor and stator. The gap width is sufficiently small (d ≈ 0.5mm) in comparison to the cylinder diameter (d ≈ 48 mm) so that to a good approximation a *plane* Couette flow with a *constant transverse* (or

shear) gradient (cf. eq. (1)) up to $\dot{\gamma} \approx 12\ 500\ s^{-1}$ can be realized in the annulus (sample volume $\approx$ 4.5 ml). The inner, static cylinder is temperature controlled.

The Couette type shear apparatus has become routine equipment for SANS experiments with sheared polymeric and colloidal systems. Moreover, similar flow cells (which fulfill special requirements, such as a variation of the shear gradient direction with respect to the direction of the primary neutron beam or an air-tight flow cell for investigation of volatile liquid systems) had been constructed by other groups and is successfully used at the ILL SANS instruments (Thurn et al., 1984; Johnson et al., 1988; Cummins et al., 1990).

Other types of flow can be distinguished from Couette flow and might be of experimental relevance either in pure form or in combination. For instance, *elongational* flow with a *longitudinal* gradient $\dot{\varepsilon}$ is best illustrated by a liquid flowing from an orifice in the bottom of a vessel due to the action of a gravitational field. On the other hand, pure *shear* flow with a *transverse* velocity gradient is realized when a fluid streams through a tube at constant flow rate. The velocity at the tube wall is zero and increases towards the centre of the tube. The parabolic velocity profile (*Poiseuille flow*), causes a non constant, transverse flow gradient which linearly decreases from its maximum value at the tube wall to zero in the central tube axis. Poiseuille type experiments are being performed both with a quartz tube flow apparatus for SANS measurements with drag reducing, rod-like micellar solutions under laminar and turbulent flow conditions (Lindner et al., 1990) as well as with a quartz slit die apparatus for measurements with flowing concentrated polymer dispersions (Laun et al., 1992).

2. Scattering experiment

2.1. EXPERIMENTAL PARAMETERS

2.1.1. *Differential scattering cross section and contrast.* In structural studies of solutions of polymers and colloids the *elastic coherent scattering process* with approximately zero energy transfer is of interest. As a function of the momentum transfer q:

$$q = |k - k_0| = \frac{4\pi}{\lambda} \cdot \sin(\theta) \tag{2}$$

and the concentration c of the solute, the scattering intensity of a solution:

$$I = f(q,c) = C \cdot \frac{d\Sigma}{d\Omega}(q,c) \tag{3}$$

is observed on the detector. k_0 and k are the momentum of the incident and scattered beam, λ is the wavelength of the radiation and 2θ is the scattering angle. C is a constant for a given experimental configuration and contains instrumental parameters (sample-to-detector distance L, primary beam intensity I_0 and area of sample diaphragm ΔA), as well as sample parameters (sample transmission T and sample thickness d). The differential scattering cross section $d\Sigma/d\Omega$ per unit sample volume ($d\Sigma/d\Omega$ is usually given in absolute units as $[cm^{-1}]$) is the probability of a quantum or particle of the primary beam with intensity I_0 to be scattered by a volume element of the illuminated sample into a solid angle element $d\Omega$ of the detector. ($d\Sigma/d\Omega$) is a sum of two terms:

$$(d\Sigma/d\Omega)^{tot.}\ [cm^{-1}] = f(q,c) = (d\Sigma/d\Omega)^{coh.} + (d\Sigma/d\Omega)^{backg.} \tag{4}$$

where $(d\Sigma/d\Omega)^{coh.}$ is the coherent differential scattering cross section containing all the information needed to describe the structure of the solute (e.g. a polymer dissolved in a solvent). $(d\Sigma/d\Omega)^{backg.}$ is a flat background due to the scattering of the solvent and the incoherent scattering of the polymer. It has to be carefully determined by an appropriate measurement (Rawiso et al., 1987; Cotton 1991).

Considering for a moment only scattering from a solution where inter-molecular interactions of the dissolved particles cancel each other out (A_2=0, see also part 2.1.3.), the coherent differential scattering cross section $(d\Sigma/d\Omega)^{coh.}$ can be written as:

$$\frac{d\Sigma^{coh.}}{d\Omega} = c \cdot K \cdot M \cdot P(q) \tag{5}$$

where c is the mass concentration of solute [g cm^{-3}], M is its molecular mass [g mole^{-1}], K is the scattering constant [cm^2 mole g^{-2}] and P(q) is the single particle form factor, containing the complete information on the conformation (shape and size) of the dissolved particle. The scattering constant K is proportional to the square of the contrast Δb [cm g^{-1}]. For *neutron scattering* with macromolecular samples, where the monomer unit is considered as the elementary scatterer, the contrast itself is given by the square of the differences of the scattering lengths b of 1g of solute particles with respect to the solvent molecules in the same volume (specific scattering length difference).

The coherent scattering lengths of nuclear isotopes are tabulated in standard references (Koester et al., 1981; Marshall et al., 1971). The large difference in scattering lengths b for the hydrogen-isotopes ^{1}H (b = - 0.374$\circ$10^{-12} cm) and ^{2}H (b = + 0.668$\circ$10^{-12} cm) is the reason why polymeric and colloidal systems with their large hydrogen content provide an excellent contrast in neutron scattering experiments when one of the components (either solvent or solute) is deuterated (isotopic labelling by chemical exchange of ^{1}H against ^{2}H). It is assumed that isotopic substitution generally does not alter the chemical properties of the system.

Formula (5) for the differential scattering cross section is valid for X-ray and light scattering experiments as well. The *only* difference is the scattering constant K which contains the characteristic contrast for the each type of radiation:

	neutrons	X-rays	light
contrast :	difference of scattering lengths b	difference of electron density ρ_e	refractive index increment $\frac{\delta n}{\delta c}$
scattering constant :	$K \propto \Delta b^2$	$K \propto \Delta\rho_e^2$	$K \propto \left[\frac{\delta n}{\delta c}\right]^2$

2.1.2. Data reduction from SANS experiments (isotropic spectra). The scattering intensity at SANS instruments is usually recorded on a position sensitive (two dimensional) multidetector (e.g. a BF$_3$ detector with 64 x 64 cells of resolution 1cm^2 at the instrument D11 of ILL, cf. Fig. 1). Standard treatment of *isotropic* SANS data (i.e spectra where the intensity distribution does not depend on the azimuthal direction) invokes a routine procedure which starts with the radial regrouping (circular averaging) of the intensity in fixed steps Δr around the centre of the primary beam, x_0, y_0. According to the experimental conditions (neutron wavelength λ and sample-to-detector distance L) an average q-value is attributed to each radius vector r on the detector:

$$q = \frac{4\pi}{\lambda} \cdot \sin[\frac{1}{2} \text{ arctg}(\frac{|r|}{L})] \tag{6}$$

The resulting intensity distribution $I_s=f(q,c)$ is corrected for absorption, sample thickness d and electronic or guide hall background $I(q)_{Cd}$. The scattering from the empty sample container (empty cell) $I_{ec}(q)$ is treated in the same way and is then subtracted from the sample scattering. Normalization to the unit incident flux, geometrical factors and detector cell efficiency corrections are performed by using the scattering $I(q)_{H2O}$ of a 1mm thick H_2O sample. Data can be put on an absolute scale by introducing the apparent differential scattering cross section per unit volume of H_2O, known from instrumental calibrations using various standard samples.

As a final result the scattering cross section of the solution per unit volume of the sample (cf. eq. (4) and (5)) is given as:

$$\left[\frac{d\Sigma}{d\Omega}\right]_{solution} [cm^{-1}] = \left[\frac{\left[\frac{I(q,c)_s-I_{Cd}}{T_s} - \frac{I_{ec}-I_{Cd}}{T_{ec}}\right]/d_s}{\left[\frac{I_{H_2O}-I_{Cd}}{T_{H_2O}} - \frac{I_{ec}-I_{Cd}}{T_{ec}}\right]/d_{H_2O}}\right] \circ \left[\frac{d\Sigma}{d\Omega}\right]^{1mm}_{H_2O} \qquad (7)$$

with T being the primary beam transmission of the solution, the H_2O sample and the empty sample container with respect to the direct beam. $d\Sigma/d\Omega^{coh.}$, the coherent differential scattering cross section of the solute, is then calculated by subtracting the flat background cross section $d\Sigma/d\Omega^{backg.}$.

The procedure shown above for determination of the concentration and q-dependent differential scattering cross section of the solute, $d\Sigma/d\Omega^{coh.}=f(q,c)$, in absolute units of $[cm^{-1}]$ from the measured intensity $I=f(q,c)$, is, although often used, based on some assumptions and simplifications, such as disregarding density fluctuations and multiple scattering as well as inelastic scattering effects. Furthermore, the problem of the smearing of the data due to the experimental geometry (slit width and detector resolution) and the wavelength spread $\Delta\lambda/\lambda$ of the neutron beam are not discussed here due to lack of space. The critical reader is explicitly invited to pay attention to these problems as they might considerably bias the quality of the results (e.g. Cotton, 1991 and references therein).

2.1.3. *Data reduction from anisotropic SANS experiments.* As a result of a SANS experiment under non-equilibrium conditions, an azimuthally anisotropic intensity distribution $I=f(x,y)$ is usually obtained on the 2-dimensional multidetector, as discussed later for the example of sheared polymer solutions (see chapter 3.). One way of treating those data is by successive sector masking of detector cells with variation of the sector opening angle $\Phi_{\perp, \parallel}$ in the preferential directions parallel and perpendicular with respect to the imposed constraint, such as the flow direction in a shear experiment for instance. For each sector, the intensity is grouped and normalized as described in part 2.1.2., yielding the differential scattering cross section as a function of $\Phi_{\perp, \parallel}$, $d\Sigma/d\Omega=f(q, \Phi_{\perp, \parallel})$. The apparent conformation parameters, such as the radius of gyration, can then be determined directly (see section 2.2.4.) for each sector mask, followed by interpolation to $\Phi_{\perp, \parallel}$ -> 0. An equivalent approach is to perform a linear extrapolation of the cross section to $\Phi_{\perp, \parallel}$ -> 0 first and to determine the conformation parameters from this extrapolation (Lindner & Oberthür, 1985).

Another way of data treatment consists of a 2-dimensional analysis of the multidetector spectra. Cell-by-cell correction and normalization yields the two-dimensional scattering cross section $d\Sigma/d\Omega=f(q_x,q_y)$. If the scattering object is characterized in real space by an eccentricity ε, such as a deformed polymer coil with ellipsoidal shape defined by the ratio of radii of gyration $R_\perp/R_\parallel$ in directions perpendicular and parallel with respect to the deformation axis, the resulting scattering pattern in reciprocal space will also have elliptical symmetry for $qR_\parallel < 1$. In this case an elliptically scaled momentum transfer q^* can be defined which allows elliptical averaging of the two dimensional intensity along $q^*=const.$ with the eccentricity ε and the radius of gyration $R_\parallel$ as fitting parameters (Mildner, 1983; Reynolds & Mildner, 1984). A further possibility of analysing 2-d data sets is a Fourier analysis which allows reconstruction of the 2-d pattern for any symmetry by Fourier series expansion of the intensity (Lindner & Hess, 1989).

2.2. SCATTERING FROM POLYMER SOLUTIONS

2.2.1. *Conformation and scattering function*. Due to restrictions in space this chapter cannot provide a detailed description of the variety of synthetic and natural polymers. A basic knowledge of their structure is taken for granted. The building block of a polymer is the monomer unit. The chain with molecular mass $M=N \cdot M_0$ is formed by chemically linking together N monomer subunits with mass M_0. The chain is thus formed by strong covalent bonds. The local flexibility of a chain, on the length scale of the monomer unit, is governed by the potential energy of rotation around chemical bonds. Beyond a characteristic distance b along the chain, the time averaged distance distribution between two monomer units loses its local character and starts to obey Gaussian statistics. The distance b, called the statistical chain element, is a measure of the chain flexibility, it is of the order of $b \approx 3$ nm for polystyrene. The overall size of the polymer coil can be characterized by its radius of gyration, R_g which is defined as the mean square of the second moment of mass distribution in the chain:

$$\langle R_g^2 \rangle = \left\langle \frac{\sum_i m_i r_i^2}{\sum_i m_i} \right\rangle \tag{8}$$

For a detailed synopsis of the different chain models for "Gaussian" coils in the "unperturbed" state as well as for "perturbed" coils (see 2.2.3.), of their corresponding scattering functions, of problems such as polydispersity effects arising with "real" samples and of limitations in the information obtained with a scattering experiment due to finite chain lengths, the reader is referred to standard textbooks and specialized reviews (e.g. Kirste & Oberthür, 1982; Ragnetti & Oberthür, 1986).

For illustration of the following paragraphs, only the typical asymptotes of the most general case of a polymer chain scattering function are presented (see Fig. 5). The orientationally averaged single particle scattering function P(q), which contains the complete information on the conformation of the scattering object, can be calculated according to the Debye's general scattering formula (Debye, 1915):

$$P(q) = \frac{1}{N^2} \cdot \sum_i \sum_j \left\langle \frac{\sin qr_{ij}}{qr_{ij}} \right\rangle \tag{9}$$

with N being the total number of scattering centres , r_{ij} their mutual distance and q being the momentum transfer during the scattering process (see section 2.1.1. and eq. (2)). The shape of the function P(q) depends on the spacial arrangement of the scattering centres as well as on their individual shape. At sufficiently low q, the shape of the particle has no influence on P(q) ("Guinier approximation", Guinier, 1939) and yields as a result of a series expansion:

$$\lim_{q \to 0} P(q) = 1 - \frac{\langle R^2 \rangle q^2}{3} \pm \dots \tag{10}$$

which allows to determine the size of the particle $\langle R \rangle$ without any further information on its shape. An analytical solution of eq. (9) is possible when the distance distribution of the scattering centres is known. For a Gaussian distribution of all the intersegmental distances the scattering function of an unperturbed, coiled structure can be written as (Debye, 1947):

$$P(q) = \frac{2 \cdot (e^{-x} + x - 1)}{x^2} \tag{11}$$

with $x = <R_g^2> \cdot q^2$, $<R_g^2>$ being the mean square radius of gyration of the coil. This function is exactly valid only for $N \to \infty$.
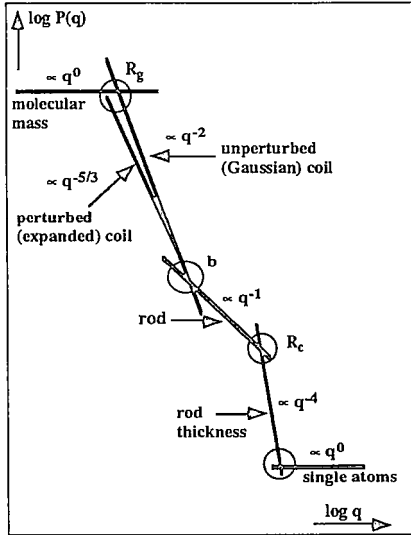

Figure 5.
Asymptotic behaviour of the scattering of a polymer chain (schematically).
Circles denote the transition regions.

The asymptotic behaviour of this function is (i) $P(q) \propto q^0$ for $q \to 0$ and (ii) $P(q) \propto q^{-2}$ for $q \to \infty$. In the case of a "perturbed" coil in a solution with excluded volume effect, the large q asymptote is characterized by $P(q) \propto q^{-5/3}$. The structure of a *real* polymer chain, however, appears on a small length scale, at distances $< b$ (statistical chain element), as a stiff, rodlike particle rather than that of a flexible coil. The scattering function of a thin rod with infinite length L is characterized by an asymptotic behaviour $P(q)' \propto q^{-1}$ for large q (Kirste & Oberthür, 1982). With increasing q, a deviation from the large q asymptote of eq. (11) is thus obtained. At still higher valus of q, the particular structure of the polymer chain with its finite thickness (atoms bound directly to the chain and molecules with a higher probability density near to the chain) becomes important, and an axial radius of gyration $<R_{ax}>$ can be defined, leading a further deviation of $P(q)$ from the q^{-1}-asymptote (see Fig. 5). It is worth pointing out, however, that the experimental determination of the asymptotic behaviour can be quite difficult, in particular the transition from the coil to the rod scattering is often not very sharp (Kirste & Oberthür, 1982).

2.2.2. *Dilute and semidilute concentration range.* A polymer solution is called *dilute* when the dissolved polymer coils are well separated from each other so that inter-chain contacts can be neglected; the space occupied by one polymer molecule is much smaller than the available volume. When increasing the concentration of polymer one arrives at the *overlap* concentration c^* where all the available space in the solution is occupied by polymer molecules. Taking the radius of gyration of the polymer chain, R_g, as a measure for the overall coil size, a reasonable approximation for c^* reads as

$$c^* = \frac{3 \cdot M}{4\pi \cdot R_g^3 \cdot N_A}$$

(12)

with R_g being the radius of gyration of the polymer molecule with molecular mass M and N_A being Avogadro's number. When exceeding the crossover concentration c^*, individual polymer coils are getting into contact with each other and chains start to interpenetrate. A convenient

geometrical criterion for sufficient dilution is thus the condition that the polymer mass concentration should be well below c*:

$$c \ < c^*. \tag{13}$$

At concentrations above c* (but still much lower than the concentration in the bulk) the solution is then called *semidilute*.

2.2.3. Interactions with the solvent. Two types of intersegmental interactions can be distinguished when a polymer chain is dissolved in a solvent. (i) Bond forces and (steric) hindrance of rotation are the nature of *short range* or longitudinal interactions, acting along the chain between neighbouring monomer units. These interactions depend on the specific architecture of a given polymer and are only slightly affected by the solvent. (ii) A second type of interactions is *long range* (transversal) and acting across the chain independently of the separation distance of monomer units. Their nature is a combination of Born repulsion between atoms with attractional van-der-Waals forces between approaching polymer segments. Long range interactions are strongly affected by the solvent.

Based on this differentiation, a polymer chain in solution may behave in two different ways: (i) if the Born repulsion is just compensated by an attractional interaction, i.e. the long range interactions are to a first approximation cancelled, the chain is in an *unperturbed* state. The polymer solution shows a pseudo-ideal behaviour with a second osmotic virial coefficient $A_2 = 0$ (the *theta point* of polymer solutions which is analogous to the Boyle point of gases). Chains without long range interactions are also called *Gaussian coils*.

(ii) In athermic solutions the attractional van-der-Waals forces are cancelled by the solvent and the Born repulsion leads to coil expansion. This situation is called excluded volume effect. The chain is in a *perturbed* or expanded state and the second osmotic virial coefficient for the solution, A_2, is positive.

2.2.4. Scattering from dilute polymer solutions. The coherent differential scattering cross section $\frac{d\Sigma}{d\Omega}(q,c)$ (the index "coh." will no longer be used in the following chapters) of the solute in a dilute polymer solution is the quantity of interest in a SANS experiment (see part 2.1.1. with eq. (3) and (7)). Its concentration and q-dependence can be expressed as (Zimm, 1948; Flory & Bueche, 1958):

$$\underbrace{\frac{K{\cdot}c}{\frac{d\Sigma}{d\Omega}(q,c)} = \frac{1}{M{\cdot}P(q)}}_{\text{intra}} + \underbrace{2A_2Q_{FB}(q){\cdot}c}_{\text{inter}} + \ldots \ldots \tag{14}$$

The measured scattering cross section thus reflects an intra -and an inter-molecular part. K is the scattering constant, A_2 is the virial coefficient of the osmotic pressure series expansion. The first (intra) term on the right hand side of eq. (14) contains the single particle scattering function P(q) (describing the time averaged conformation of one isolated polymer particle, normalized to $P_{(q=0)}=1$), and its molecular mass M. The second (inter) term with the function $A_2Q_{FB}(q)$ reflects the average spatial arrangement of 2 particles during their mutual approach in the solution of concentration c and interactions of the solute and the solvent, normalized such that $Q_{FB(q=0)}=1$ and Q_{FB} $_{(q->\infty)}=0$. Hence, at sufficently large q the scattering intensity does no longer depend on concentration (Kirste & Oberthür, 1982).

The quantity which describes the scattering behaviour of one single particle is the partial differential specific scattering cross section, $\frac{d\sigma}{d\Omega}(q)$ [cm^2 g^{-1}], which is defined as:

$$\frac{d\sigma}{d\Omega}(q) = \lim_{c->0}\left[\frac{1}{c}{\cdot}\frac{d\Sigma}{d\Omega}(q,c)\right] = K{\cdot}M{\cdot}P(q) \tag{15}$$

In the case of ideal solutions $(A_2 = 0)$ $\frac{d\sigma}{d\Omega}(q)$ is directly obtained from the scattering cross section $\frac{d\Sigma}{d\Omega}(q,c)$ at a given concentration c (see eq. (4) and (5)). For athermic solutions with $A_2 > 0$ (good solvent), $\frac{d\sigma}{d\Omega}(q)$ can be obtained by an appropriate plot of the concentration dependent cross sections measured from a concentration series, $K \cdot c/ (d\Sigma/d\Omega)$, as a function of (const. $\cdot q^2 + c$), where const. is an arbitrary parameter ("Zimm" plot). This representation, which is linear at sufficiently low q, allows a simultaneous extrapolation to c=0 and q=0. From the line at c=0 one obtains:

$$\lim_{c \to 0} \frac{K \cdot c}{\frac{d\Sigma}{d\Omega}(q,c)} = \frac{1}{M_w \, P(q)} = \frac{1}{M_w}\left[1 + \frac{\langle R^2 \rangle_z \, q^2}{3} + ...\right] \qquad (16)$$

with the z-average of the radius of gyration $<R_g>_z$ resulting from the slope. The line with q=0 yields:

$$\lim_{q \to 0} \frac{K \cdot c}{\frac{d\Sigma}{d\Omega}(q,c)} = \frac{1}{M_w}[1 + 2A_2 \, M_w \, c + ...] \qquad (17)$$

with A_2 following from the slope. The ordinate intercept of both lines yields the weight average of the molecular weight, M_w. Thus, a thermodynamic analysis of the system, together with information on the shape and conformation of one isolated molecule in solution are obtained. For more details on different extrapolation methods, in particular with respect to different particle shapes, the reader is referred to the literature (e.g. Kirste & Oberthür, 1982; Ragnetti & Oberthür, 1986).

2.2.5. Scattering from semidilute solutions.

A semidilute polymer system can be characterized by a correlation length ξ, beyond which the chains are interpenetrated and the polymer concentration is nearly homogeneous. ξ is also the average distance between interchain contact points. In terms of the blob-picture (DeGennes, 1979), the semidilute solution can be represented as a collection of uncorrelated chain segments of size ξ ("blobs"). When a contrast is established between the polymer and the solvent (such as dissolving a deuterated polymer in a protonated solvent), the neutron scattering intensity $d\Sigma/d\Omega(q)$ follows an Ornstein-Zernike law for $\xi q \ll 1$:

$$\frac{d\Sigma}{d\Omega}(q) = \frac{\frac{d\Sigma}{d\Omega}(q=0)}{(1 + \xi^2 \, q^2)} \qquad (18)$$

ξ is the correlation length scale beyond which ($\xi q < 1$) the elementary segments of the chains can be considered as randomly distributed; on length scales larger than ξ correlations along any given chain are screened out. The scattering intensity of a semidilute solution can be related for $\xi q < 1$ to the dynamical fluctuations of the polymer concentration. At larger q values, for $\xi q > 1$, the intensity follows a cross over towards a power law

$$\frac{d\Sigma}{d\Omega}(q) \propto q^{-D_f} \qquad (19)$$

where $D_f = 5/3$ in the good solvent regime and $D_f = 2$ in the theta domain.

3. Applications: SANS from *sheared* polymer solutions

The behaviour of dilute and semidilute polymer solutions in the *quiescent* state has been extensively studied during the past two decades by scattering techniques such as SANS (e.g. Farnoux et al., 1975; Daoud et al., 1975; Daoud et al., 1976; Farnoux et al., 1978; Richards et al., 1978; Ullman et al., 1985; King et al., 1985; Rawiso et al., 1987). The technique, resolving the range of momentum transfer q in the polymer scattering curve from length scales of the order of the overall coil size to the scattering of the flexible segment, is a particularly suitable method for obtaining information on the statistical conformation of polymer molecules in dilute solution as well as on the structure of entangled systems in the semidilute concentration range. This chapter describes some experimental results obtained with *flowing* polymer solutions in the dilute regime. In particular, the method of small angle neutron scattering in conjunction with laminar Couette shear flow in a scattering geometry as sketched in Fig. 4 has been applied.

Fig. 6 shows a schematic temperature-concentration phase diagram as being provided by renormalization group theory for a description of polymer solution behaviour (Daoud & Jannink, 1976). For further details the reader is referred to standard references. For comparison, the experimental conditions of some different shear experiments which have been reported so far, are indicated. The hatched part 1 is the dilute region under good solvent and theta conditions where SANS experiments (described partly in this chapter) have been performed (Lindner & Oberthür, 1988). Hatched part 2 indicates the region of SANS experiments with semidilute polystyrene solutions (Boué & Lindner, 1994, Boué & Lindner, 1995). The points 3 (Hammouda, Nakatani, Waldow & Han, 1992), 4 (Hashimoto & Fujioka, 1991, Hashimoto & Kume, 1992), 5 (van Egmond, Werner & Fuller, 1992) and 6 (Wu, Pine & Dixon, 1991) indicate experimental conditions of other works using light scattering and SANS. Experiments 1 and 4 - 6 have been rescaled to equivalent temperatures (temperature given on the right side of the diagram, $(T_i-\Theta)*$) with respect to SANS experiments (Boué & Lindner, 1994).
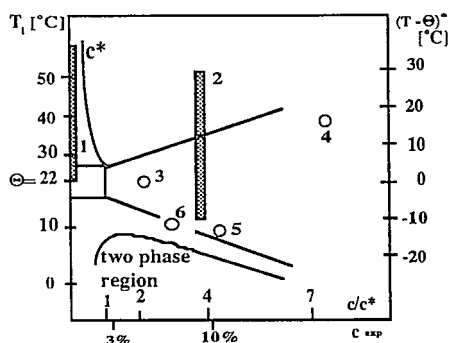

Figure 6. Schematic temperature-concentration diagram for polymer solutions together with different experimental conditions for shear experiments with polystyrene (see text).

3.1. POLYMER CONFORMATION IN SHEARED, DILUTE SOLUTION

Under laminar shear flow conditions, information about the morphological changes on the molecular level are of fundamental importance for an understanding of the macroscopic properties of the flowing system. To what extent is the conformation of a single and more or less flexible polymer chain altered by the velocity gradient in the streaming solution, as sketched for example in Fig. 2 ?

A distortion of the polymer coil conformation in flow has long been predicted by theory. In a longitudinal gradient $\dot{\varepsilon}$ a sharp coil-stretch transition should occur for $\dot{\varepsilon}\tau \geq 1$, where τ is the

largest relaxation time of the intra-molecular chain motion (DeGennes, 1974), whereas in a transverse (or constant shear) gradient $\dot\gamma$ a gradual transition towards an anisotropic intersegmental distance distribution is expected with increasing shear gradient (Peterlin et al., 1958). A common feature of the different theoretical treatments of the ideal flexible chain molecule in shear flow is to consider the balance of (i) frictional forces, (ii) contractile forces and (iii) Brownian motion of the chain segments. The friction forces acting on the polymer chain segments in the shear gradient result in a combined rotation and deformation of the coil beside the translative motion in flow direction, whereas the elastic properties of the chain resist a change of the shape to less probable chain conformations. According to the theories, the coil shape is deformed in shear flow and changes to an anisotropic conformation with the symmetry of an ellipsoid of rotation. A dynamic effect, however, limits the deformation of the single coil in shear flow: shape changes require changes in chain conformation, e.g. intra-molecular bond rotations which are hindered by local energy barriers.

With *scattering* techniques it is possible in principle to observe the overall molecular dimensions *directly* and to probe the chain extension of a single macromolecule under flow conditions.
3.1.1. *Good solvent conditions*. In particular, the shear-induced deformation of polystyrene in dilute solution has been systematically studied by SANS experiments in laminar shear flow at the ILL. Considering the q-dependent dynamics of a single polymer coil in solution, experimental conditions for shear induced deformation can be roughly estimated (Lindner & Oberthür, 1985): the interaction between shear gradient $\dot\gamma$ and the longest segmental relaxation time τ_{max} of the polymer chain implies the condition

$$\dot\gamma\,\tau_{max} \geq 1 \tag{20}$$

for a permanent distortion of the chain conformation in shear flow. It turns out that by *increasing* the solvent viscosity the segmental relaxation can be slowed down such that relationship (27) is fulfilled and shear deformation can be observed under given experimental conditions with SANS measurements.
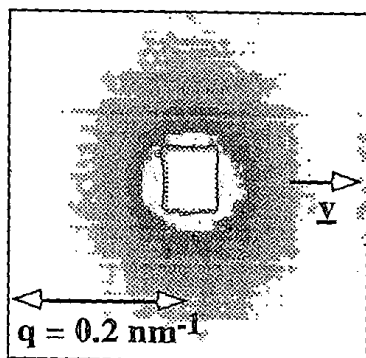

Figure 7. SANS pattern (raw data) of a dilute polymer solution in a good solvent (polystyrene, M_w=280000g/mole, solvent oligostyrene+toluene, solvent viscosity η=50 mPas, polymer concentration c=8 g/ L) measured at D11 of the Institut Laue-Langevin, Grenoble. Solution in laminar shear flow at a gradient of $\dot\gamma$ =6000 s^{-1} (the light rectangle in the middle of the detector is due to the primary neutron beam stop).

The mixture of oligostyrene (OS, M_w=800 g/mole, M_w/M_n=1.3) with toluene is a suitable viscous solvent, its viscosity can be adjusted by variation of the composition (OS content). This solvent mixture is a thermodynamically good solvent for polystyrene. Concentration series of fully deuterated polystyrene samples with low polydispersity (PS-d, prepared by anionic polymerization) at different molecular masses in the range M_w= 160000 to 500000 gmole^{-1} were prepared in the dilute concentration range (1.5 $\leq$ c [g/ L] $\leq$ 8). The combination of the perdeuterated polymer with protonated solvent provides sufficient scattering contrast in neutron scattering experiments. Shear experiments were performed at the SANS instrument D11 of the Institut Laue-Langevin in a q-range of 0.05 < q/ nm^{-1} < 1.80, using the Couette-type shear apparatus at various shear gradients up to $\dot\gamma$ = 8500 s^{-1} (Lindner & Oberthür, 1988).

Figure 7 shows as one example the uncorrected two dimensional SANS spectra of a dilute polystyrene solution (molecular mass 280000 g/mole, mass concentration of polymer c=8 g/ L) measured in laminar shear flow. The SANS intensity of the solution at rest (data not shown) is azimuthally isotropic, whereas the sheared polymer solution (Fig. 7) shows an anisotropic intensity distribution on the 2d-multidetector with elliptical symmetry (long axis perpendicular with respect to flow direction). Moreover, the magnitude of the effect depends upon molecular mass, shear gradient, solvent viscosity and q-range.

The SANS spectra of the dilute solutions at rest and under shear were treated according to standard procedures (see chapter 2.1.2. and 2.1.3.). The (anisotropic) two-dimensional multidetector data have been radially grouped in the preferential directions parallel (||) and perpendicular (⊥) with respect to the flow direction in the gap of the flow cell. Normalization and extrapolation to zero concentration yields the normalized scattering curve for a single polystyrene chain in dilute solution as shown in Figure 8.
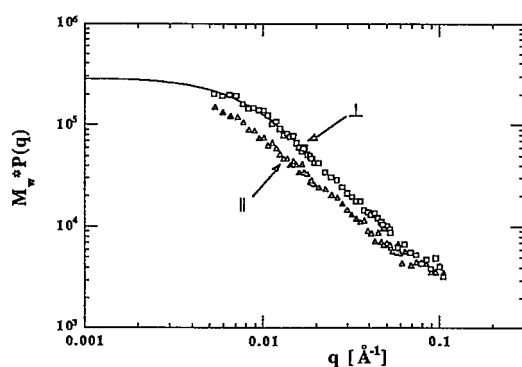

Figure 8.
Normalized scattering curve $M_w \cdot P(q)=f(q)$ of polystyrene (M_W=280000 g/ mole, good solvent) in a shear gradient of $\dot\gamma = 6\ 000\ s^{-1}$, evaluated in the directions perpendicular (⊥) and parallel (||) to the flow direction. The drawn line corresponds to the scattering curve of the polystyrene in the quiescent state (the momentum transfer q is given in units of [Å^{-1}], 1 Å^{-1} = 10 nm^{-1}).
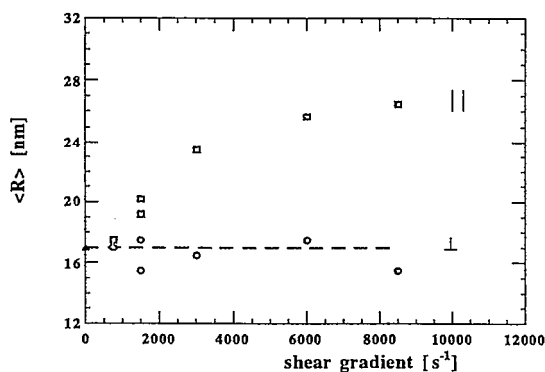

Figure 9.
Experimental radii of gyration as determined from the solution at rest (<R_{iso}>, filled triangle) and from the sheared solutions (<$R_\perp$> : filled circles, <$R_{||}$>: filled squares) as a function of shear gradient $\dot\gamma$.

A distinct anisotropy, already visible in the uncorrected, two-dimensional detector pattern (cf. Fig. 7) is observed in the region of small values of the momentum transfer q, where the length

scale of the radius of gyration (a measure of the overall molecular size of the polymer coil) is examined. The anisotropy of the formfactor decreases with increasing momentum transfer q.

The cross-over to isotropic scattering (with respect to the directions parallel and perpendicular) which is observed at large q-values shows that the *short range* distribution of chain segments, on the length scale of the statistical chain element, is not affected by the flow field.

Figure 9 shows the experimental radii of gyration, resulting from the low q region, as a function of the various shear gradients $\dot{\gamma}$ applied to the polystyrene solution. The value $<R_{||}>$ increases significantly with increasing shear gradient $\dot{\gamma}$, whereas the value $<R_\perp>$ is within experimental error identical to the radius of gyration of the unsheared polystyrene $<R_{iso}>$ and independent of $\dot{\gamma}$.
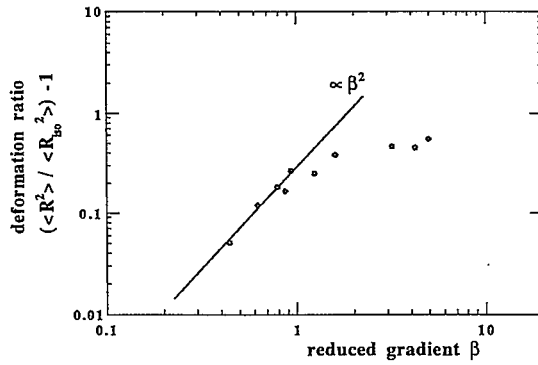

Figure 10.
Experimental deformation ratio $(<R^2> / R_{iso}^2>)-1$ as a function of the reduced gradient β. The β^2-dependence (continuous line) is predicted for an infinitely flexible coil for the Rouse as well as for the Zimm model.

Based on the experimental radii of gyration, the deformation ratio of the polystyrene chain,

$$\frac{<R>}{<R_{iso}>} - 1 \quad , \qquad (21)$$

can be calculated as a function of the reduced shear gradient

$$\beta = \frac{[\eta]\, \eta_s\, M_w\, \dot{\gamma}}{R\, T} \qquad (22)$$

(cf. Figure 9). $<R>$ and $<R_{iso}>$ are the radii of gyration of the deformed coil and of the coil in solution at rest respectively; $[\eta]$ is the intrinsic viscosity, η_s is the solvent viscosity and R is the gas constant (the other symbols have the usual meaning). The reduced gradient β is a dimensionless orientation variable for rescaling the different experimental conditions (e.g. molecular mass M_w, solvent viscosity η_s and shear gradient $\dot{\gamma}$). The gradient dependence of the deformation ratio (cf. Figure 10) allows quantitative comparison with theoretical predictions for shear deformation of a single polymer coil, including the effect of a limitation of dynamic flexibility. An *ideal flexible* behaviour with a β^2 dependence is only found at low gradients whereas with increasing β, the deformation of the polymer chain is found to be smaller than for a dynamically infinitely flexible molecule, in qualitative agreement with theory (Lindner & Oberthür, 1988).

Recently, a N-bead chain of N monomers (N≤50) in a solvent subjected to shear flow has been treated by non equilibrium molecular dynamics (NEMD) in a computer simulation (Pierleoni & Ryckaert, 1995). Results are consistent with the above described SANS data for polystyrene in good solvent conditions.

3.2. FURTHER EXAMPLES

3.2.1. *Theta solvent conditions*. An investigation of the dilute polymer-solvent system under shear close to the theta point (second osmotic virial coefficient $A_2=0$) is not only interesting with respect to a check of the theoretical predictions concerning the overall coil deformation. The thermodynamic response under non-equlibrium conditions is a further point of interest. An increasing theta temperature under shear, due to the externally applied shear force, has been predicted theoretically in terms of a decrease of excluded volume due to intersegmental interaction (orientation and deformation of the chain) (Sariban, 1986). Shearing of the polymer system is, however, not equivalent to a simple effective temperature shift but involves a more complicated interplay between hydrodynamic and thermodynamic effects. For instance, shear induced *mixing* has been observed in polymer blends with an apparent shift of the phase boundary only in direction parallel to the flow (Nakatani et al., 1990).

Recent SANS experiments at D11 under shear (Lindner, 1996) confirm earlier findings with a solution of perdeuterated polystyrene in the theta solvent di-(octylphthalate). At a temperature of $T\approx22°C$ (which is the theta temperature for this polymer-solvent system) and at shear gradients below $\dot{\gamma}\approx5000$ s^{-1}, an anisotropic scattering pattern, i.e. a gradient-dependent chain deformation, is observed as in the good solvent case. At higher shear gradients, however, above a critical shear gradient of the order of $\dot{\gamma}\approx5000$s^{-1}, in addition to the anisotropy in the intermediate q-range, a (reversible) *increase* of the scattering intensity is observed in the low q-range. A similar result, but without observation of a scattering anisotropy had been found by Hammouda et al. (Hammouda et al., 1992). Further experiments are necessary to elucidate the physical origin of these results, either in terms of shear enhanced density fluctuations (Helfand et al., 1989, Milner, 1991) or in terms of shear induced phase separation based on thermodynamic arguments (Rangel-Nafaile et al., 1984).

3.2.2. *Flow enhanced concentration fluctuations in sheared, semidilute polymer solutions*. A very recent subject of theoretical and experimental interest is scattering studies of polymers in sheared *semidilute* solutions (Larson, 1992). It is intuitively clear that the situation is more complex than in the case of dilute solutions where single chain behaviour is observed: with increasing polymer concentration the deformation of the polymer coil in flowing solution is increasingly influenced by imposed topological constraints due to molecular entanglements. Above the overlap concentration c* (cf. eq. (12)) the chains form a three dimensional transient network via entanglements that extend throughout the solution. During flow the network is stretched but also continuously regenerated.

Using light scattering (LS) and SANS with various scattering geometries (different beam paths with respect to the shear gradient direction) and shear flow geometries (Couette or cone-and-plate), it has been observed by several groups that the scattering intensity of a semidilute solution is strongly increased by shearing the system. It should be stressed at this point that LS and SANS differ by about an order of magnitude in the range of momentum transfer q of the experiment. SANS, on the higher q side, explores shorter length scales in the system (ranging from $q\xi < 1$ to $q\xi >> 1$, ξ being the correlation length in the quiescent solution) as compared to LS. Flow enhanced concentration fluctuations have been found to be either anisotropic with respect to the flow direction (Wu et al., 1991; van Egmond et al., 1992; Hashimoto et al., 1991; Hashimoto et al., 1992, Boué & Lindner, 1994, Boué & Lindner, 1995) or to be isotropic (Hammouda et al., 1992). A debate is centred around the question whether shear induces a shift in the cloud point of the solution or whether the concentration fluctuations in the entangled polymer system are amplified and distorted by other mechanisms, *without* a shift in the critical temperature for phase separation (cf. Fig. 6).

Fig. 12 shows the result of a recent experiment obtained at D11 of the ILL Grenoble, at lowest q-values down to 8×10^{-4} Å^{-1} (Boué & Lindner, 1996). Under shear, the scattering is slightly

anisotropic at large momentum transfer q, with a long axis perpendicular to the flow direction. At low q, closer to the beamstop, a different feature compared to the scattering of the sheared *dilute* solution (cf. Fig. 7) is observed; a pronounced increase *parallel* to the flow direction leads to a double winged shape ("*butterfly pattern*") already observed in deformed gels, rubbers and in polymer melts (Mendès et al., 1991; Bastide et al., 1988; Boué et al. 1991). The effect is increasing with increasing shear.
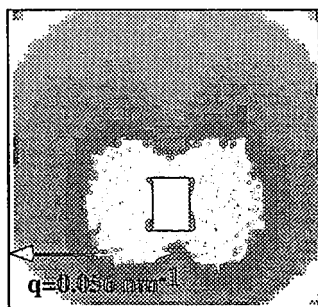

Figure 12. SANS "butterfly" pattern (raw data) of a semidilute polymer solution (polystyrene, M_w=514000 g/mole, solvent Di-octylphthalate, concentration 97 g/L ($\approx$ 9% w/w), temperature T=22°C), measured at D11, ILL, Grenoble (detector distance L=35.7m, wavelength λ=10Å).
Solution in laminar shear flow at a gradient of $\dot{\gamma}$ =150 s^{-1} (the light rectangular spot in the middle of the detector is due to the primary neutron beam stop).

Several theoretical concepts have tried to explain the shear induced enhancement of concentration fluctuations at low q as experimentally observed with LS and SANS measurements (e.g. Rangel-Nafaile et al., 1984, Helfand & Fredrickson, 1989; Onuki, 1990, Milner, 1991).

A possible approach considers disinterpenetration of an assembly of regions of higher concentrations and regions of lower concentrations in the solution (Bastide et al., 1990), as proposed for the description of percolation clusters of regions of high crosslinking ratio after random crosslinking of a semidilute solution, which is well suited to predicting the "butterfly effect" in uniaxially deformed swollen gels as observed with SANS (Mendès et al., 1991). The deformation in the parallel direction acts as a dilution of the high concentration regions (harder) inside the low concentration regions (softer). These regions may be highly "interpenetrated" in the *quiescent* state, i.e. their screening length ξ (observable by scattering) is much smaller than their maximum size. Dilution, as equivalent for instance to shear in parallel direction, will increase the "visible" size of the clusters. The model of disinterpenetration of frozen heterogeneities is also proposed to explain light scattering results with sheared semidilute polymer solutions (Hashimoto et al., 1992).

The phenomenon is, however, not restricted to polymeric systems (melts, rubbers, gels and semidilute solutions). Flow enhanced concentration fluctuations are observed for instance also with lyotropic lamellar phases (Weigel et al., 1996, Lindner et al., 1997).

4. Summary

Neutron scattering is a most convenient technique for studying changes of the microscopic structure when the system is in a non-equilibrium state such as shear flow. In soft condensed matter research this type of experiments is attracting increasing attention because of their technological implications; combining a classical scattering method with an externally applied field, important information is obtained, for instance, about structural changes of deformable or anisotropic particles with respect to shape and size, on dynamic properties as well as on thermodynamic behaviour.

5. References

Alexander, L.E. (1985). *X-ray Diffraction Methods in Polymer Science*, Malabar: Robert E. Krieger

Baruchel, J., Hodeau, J.L., Lehmann, M., Regnard, J.R., Schlenker, C. (1993). *Neutron and Synchrotron Radiation for Condensed Matter Studies*. Berlin: Springer

Bastide, J., Buzier M., Boué, F. (1988). *Springer Proceedings in Physics* **29**, 112-120

Bastide, J., Leibler, L., Prost, J. (1990). *Macromolecules* **23**, 1821

Bird, R.B., Armstrong, R.C., Hassager, O. (1977). *Dynamics of Polymeric Liquids*, New York: John Wiley

Boué, F. (1987). *Adv. Pol. Sci.* **82**, 47-101

Boué, F., Bastide J., Buzier M., Lapp, A., Herz, J., Vilgis, T.A. (1991). *Colloid Polym. Sci.* **269**, 195-216

Boué, F., Lindner, P. (1994). *Europhysics Letters* **25**, **6**, 421

Boué, F., Lindner, P. (1995). In Nakatani, A.I., Dadmun, M.D. (eds.) *Flow Induced Structure in Polymers*, ACS Symposium Series 597. Washington: ACS

Boué, F., Lindner, P. (1996) unpublished results

Brumberger, H. (1995). *Modern Aspects of Small Angle Scattering*. Dordrecht: Kluwer

Chen, S.H., Chu, B., Nossal R. (eds) (1981). *Scattering Techniques Applied to Supramolecular and Nonequilibrium Systems*, NATO Advanced Study Institutes Series B: Physics, Vol. 73, New York: Plenum Press

Cotton, J.P. (1991). In Lindner, P., Zemb, Th. (eds.) *Neutron, X-ray and Light Scattering: Introduction to an Investigative Tool for Colloidal and Polymeric Systems*. Amsterdam: North Holland

Cummins, P.G., Staples, E., Millen, B., Penfold, J. (1990). *Meas. Sci. Technol.*, **1**, 179

Daoud, M., Cotton, J.P., Farnoux B., Jannink G., Sarma G., Benoit H., Duplessix R., Picot C., DeGennes, P.G. (1975). *Macromolecules* **8**, 804-818

Daoud, M., Jannink G. (1976). *J. Phys. (Paris)* **37**, 973-979

Debye, P. (1915). *Ann. Physik* **46**, 809-823

Debye, P. (1947). *J. Phys. Colloid. Chem.* **51**, 18-32

DeGennes, P.G. (1974). *J. Chem. Phys.* **60**, 5030

DeGennes, P.G. (1979). *Scaling Concepts in Polymer Physics*, Ithaca and London: Cornell University Press

DesCloizeaux, J., Jannink G. (1990). *Polymers in Solution*. Oxford: Clarendon Press

Doi, M., Edwards, S.F. (1986). *The Theory of Polymer Dynamics*. Oxford: Clarendon Press

Farnoux, B., Daoud, M., Decker, D., Jannink, G., Ober, R. (1975). *J. Phys. (Paris)* **36**, L35-39

Farnoux, B., Boué, F., Cotton, J.P., Daoud, M., Jannink, G., Nierlich, M., DeGennes, P.G. (1978). *J. Phys. (Paris)* **39**, 77-86

Flory, P.J. (1953). *Principles of Polymer Chemistry*, New York: Cornell University Press

Flory, P.J. (1969). *Statistical Mechanics of Chain Molecules*, Ithaca: Cornell University Press

Flory, P.J., Bueche, A.M. (1958). *J. Polym. Sci.* **27**, 219-229

Glatter, O. and Kratky, O. (eds.) (1982). *Small Angle X-ray Scattering*. London: Academic Press.

Guinier, A. (1939). *Ann. Phys.* **12**, 161

Guinier, A., Fournet, G. (1955). *Small Angle Scattering of X-rays*, New York: John Wiley

Hammouda, B., Nakatani, A.I., Waldow, D.A., Han, C.C. (1992). *Macromolecules* **25**, 2903-2906

Hashimoto, T., Fujioka, K. (1991). *J. Phys. Soc. Japan* **60**, 356

Hashimoto, T., Kume, T. (1992). *J. Phys. Soc. Japan* **61**, 1839

Helfand, E., Fredrickson, G.H. (1989). *Phys. Rev. Lett.* **62**, 2468

Higgins, J.S., Benoît, H.C. (1994) (eds.) *Polymers and Neutron Scattering*. Oxford: Clarendon Press

Ibel, K. (1976). *J. Appl. Cryst.* **9**, 296-309

Johnson, S.J., deKruiff, C.G., May, R.P. (1988). *J. Chem. Phys.* **89**, 5909

King J.S., Boyer W., Wignall G.D., Ullman R. (1985). *Macromolecules* **18**, 709-718

Kirste, R.G., Oberthür, R.C. (1982). *Synthetic Polymers in Solution* in Glatter, O. and Kratky, O. (eds.) *Small Angle X-ray Scattering*. London: Academic Press.

Koester, L., Rauch, H. (1981). *Summary of Neutron Scattering Lengths*
IAEA Contract 2517/RB

Larson, R.G. (1992). *Rheol. Acta* **31**, 497 - 520

Laun, H.M., Bung, R., Hess, S., Loose, W., Hess, O., Hahn, K., Hädicke, E., Hingmann, R., Schmidt, F., Lindner, P. (1992). *J. Rheol.* **36**(4), 743-787

Lindner, P., Oberthür, R. (1985). *Colloid Polym. Sci.* **263**, 443-453

Lindner, P., Oberthür, R. (1988). *Colloid Polym. Sci.* **266**, 886-897

Lindner, P., Hess, S. (1989). *Physica B* **156&157**, 512-514

Lindner, P., Bewersdorff, H.W., Heen, R., Sittart, P., Thiel, H., Langowski, J., Oberthür, R. (1990). *Progr. Colloid Polym. Sci.* **81**, 107-112

Lindner, P., May, R.P., Timmins, P.A., (1992). *Physica B* **180 & 181**, 967-972

Lindner, P., Oberthür, R.C. (1984). *Rev. Phys. Appl.* **19**, 759

Lindner, P., Zemb, Th. (1991). *Neutron, X-ray and Light Scattering: Introduction to an Investigative Tool for Colloidal and Polymeric Systems*. Amsterdam: North Holland

Lindner, P., (1996) unpublished results

Lindner, P., Zipfel, J., Richtering, W. (1997) ILL Annual Report

Marshall, W., Lovesey, S.W. (1971). *Theory of Thermal Neutron Scattering*. Cambridge: Oxford Clarendon

Mendès, E., Lindner, P., Buzier, M., Boué, F., Bastide, J. (1991). *Phys. Rev. Lett.* **66**, 1595

Mildner, D.R.F. (1983). *Macromolecules* **16**, 1760-1763

Milner, S. (1991). *Phys. Rev. Lett.* **66**, 1477

Morawetz, H. (1975). *Macromolecules in Solution*. New York: John Wiley

Nakatani, A.I., Kim, H., Takahashi, Y., Matsuhita ,Y., Takano A., Bauer, B.J., Han, C.C. (1990). *J. Chem. Phys.* **93**, 795

Nakatani, A.I., Dadmun, M. (1995) *Flow-Induced Structure in Polymers*. Washington: ACS

Oberthür, R.C. (1983). *Inst. Phys. Conf. Ser.* **64**, 321

Oberthür, R.C. (1984). *Rev. Phys. Appl.* **19**, 663

Onuki, A. (1990). *J. Phys. Soc. (Jpn)* **59**, 3423; **59**, 3427

Peterlin, A., Heller, W., Nakagaki, M. (1958). *J. Chem. Phys.* **28**, 470

Ragnetti, M., Oberthür, R.C. (1986). *Colloid Polym. Sci.* **264**, 32-45

Rangel-Nafaile, C., Metzner, A.B., Wissbrun, A.F. (1984). *Macromolecules* **17**, 1187

Rawiso, M., Duplessix, R., Picot, C. (1987). *Macromolecules* **20**, 630-648

Reynolds, L.E., Mildner, D.R.F. (1984). *J. Appl. Cryst.* **17**, 411-416

Richards, R.W., Maconnachie A., Allen G. (1978). *Polymer* **19**, 266-270

Pierleoni, C., Ryckaert, J.P. (1995). *Macromolecules* **28**, 5097-5108

Sariban, A. (1986) *Macromolecules* **19**, 843

Schmatz, W., Springer, T., Schelten, J., Ibel, K. (1974). *J. Appl. Cryst.* **7**, 96-116

Tanford, C. (1961). *Physical Chemistry of Macromolecules*. New York: John Wiley

Thurn, H., Kalus, J., Hoffmann, H. (1984). *J. Chem. Phys* **80**, 3440

Ullman, R., Benoit, H., King, J.S. (1986). *Macromolecules* **19**, 183-188

Van Egmond, J.W., Werner, D.E., Fuller, G.G. (1992). *J. Chem. Phys.* **96**, 7742

Weigel, R., Läuger, J., Richtering, W., Lindner, P. (1996). *J. Phys. II France* **6**, 529-542

Wu, X.L., Pine, D.J., Dixon, P.K. (1991). *Phys. Rev. Lett.* **66**, 2408

Yamakawa, H. (1971). *Modern Theory of Polymer Solutions*, New York: Harper & Row

Zimm, B. (1948). *J. Chem. Phys.* **16**, 1093-1116